

# StateMask: Explaining Deep Reinforcement Learning through State Mask

## S1 Proof of Theorem 1

Before we proving Theorem 1, we first introduce the following lemma.

**Lemma 2.** *Given an old and new policy of the state mask  $\tilde{\pi}_{\theta_{old}}$  and  $\tilde{\pi}_\theta$ , respectively, if  $\eta(\tilde{\pi}_{\theta_{old}}) \leq \eta(\tilde{\pi}_\theta) \leq 2\eta(\bar{\pi}) - \eta(\tilde{\pi}_{\theta_{old}})$ , we have  $|\eta(\tilde{\pi}_\theta) - \eta(\bar{\pi})| \leq |\eta(\tilde{\pi}_{\theta_{old}}) - \eta(\bar{\pi})|$ .*

**Proof of Lemma 2.** The monotonicity property requires  $|\eta(\tilde{\pi}_\theta) - \eta(\bar{\pi})| \leq |\eta(\tilde{\pi}_{\theta_{old}}) - \eta(\bar{\pi})|$ . The following equivalence holds:

$$\begin{aligned} & |\eta(\tilde{\pi}_\theta) - \eta(\bar{\pi})| \leq |\eta(\tilde{\pi}_{\theta_{old}}) - \eta(\bar{\pi})| \\ \iff & \eta(\tilde{\pi}_\theta)^2 - 2\eta(\tilde{\pi}_\theta)\eta(\bar{\pi}) + \eta(\bar{\pi})^2 \leq \eta(\tilde{\pi}_{\theta_{old}})^2 - 2\eta(\tilde{\pi}_{\theta_{old}})\eta(\bar{\pi}) + \eta(\bar{\pi})^2 \\ \iff & (\eta(\tilde{\pi}_\theta) + \eta(\tilde{\pi}_{\theta_{old}}))(\eta(\tilde{\pi}_\theta) - \eta(\tilde{\pi}_{\theta_{old}})) \leq 2\eta(\bar{\pi})(\eta(\tilde{\pi}_\theta) - \eta(\tilde{\pi}_{\theta_{old}})). \end{aligned} \quad (1)$$

Therefore, if  $\eta(\tilde{\pi}_{\theta_{old}}) \leq \eta(\tilde{\pi}_\theta)$  and  $\eta(\tilde{\pi}_\theta) + \eta(\tilde{\pi}_{\theta_{old}}) \leq 2\eta(\bar{\pi})$ , or in other words,  $\eta(\tilde{\pi}_{\theta_{old}}) \leq \eta(\tilde{\pi}_\theta) \leq 2\eta(\bar{\pi}) - \eta(\tilde{\pi}_{\theta_{old}})$ , we have  $|\eta(\tilde{\pi}_\theta) - \eta(\bar{\pi})| \leq |\eta(\tilde{\pi}_{\theta_{old}}) - \eta(\bar{\pi})|$ .  $\square$

Recall that Lemma 1 in Section 3.2 shows the upper bound and the lower bound of  $\eta(\tilde{\pi}_\theta)$ . An immediate implication of Lemma 1 enables us to obtain the inequalities to satisfy Lemma 2.

From Lemma 1, we can easily derive the lower bound of  $\eta(\tilde{\pi}_\theta)$  as  $\eta(\tilde{\pi}_\theta) \geq L_{\tilde{\pi}_{\theta_{old}}}(\tilde{\pi}_\theta) - C\mathbb{KL}^{\max}(\tilde{\pi}_{\theta_{old}}(\cdot | s) \| \tilde{\pi}_\theta(\cdot | s))$ . If the lower bound is greater than  $\eta(\tilde{\pi}_{\theta_{old}})$ , then we can guarantee that  $\eta(\tilde{\pi}_\theta) \geq \eta(\tilde{\pi}_{\theta_{old}})$ . Similarly, we can obtain the upper bound of  $\eta(\tilde{\pi}_\theta)$  as  $\eta(\tilde{\pi}_\theta) \leq L_{\tilde{\pi}_{\theta_{old}}}(\tilde{\pi}_\theta) + C\mathbb{KL}^{\max}(\tilde{\pi}_{\theta_{old}}(\cdot | s) \| \tilde{\pi}_\theta(\cdot | s))$ . If the upper bound is lower than  $2\eta(\bar{\pi}) - \eta(\tilde{\pi}_{\theta_{old}})$ , we can guarantee that  $\eta(\tilde{\pi}_\theta) \leq 2\eta(\bar{\pi}) - \eta(\tilde{\pi}_{\theta_{old}})$ . Putting all these inequalities together, the following inequalities are the sufficient conditions for satisfying  $|\eta(\tilde{\pi}_\theta) - \eta(\bar{\pi})| < |\eta(\tilde{\pi}_{\theta_{old}}) - \eta(\bar{\pi})|$ :

$$\begin{aligned} L_{\tilde{\pi}_{\theta_{old}}}(\tilde{\pi}_\theta) & \geq \eta(\tilde{\pi}_{\theta_{old}}) + C\mathbb{KL}^{\max}(\tilde{\pi}_{\theta_{old}}(\cdot | s) \| \tilde{\pi}_\theta(\cdot | s)) \\ L_{\tilde{\pi}_{\theta_{old}}}(\tilde{\pi}_\theta) + C\mathbb{KL}^{\max}(\tilde{\pi}_{\theta_{old}}(\cdot | s) \| \tilde{\pi}_\theta(\cdot | s)) & \leq 2\eta(\bar{\pi}) - \eta(\tilde{\pi}_{\theta_{old}}). \end{aligned} \quad (2)$$

## S2 Derivation of Eqn. (5)

First, let  $M_{\tilde{\pi}_{\theta_{old}}}(\tilde{\pi}_\theta) = L_{\tilde{\pi}_{\theta_{old}}}(\tilde{\pi}_\theta) - C\mathbb{KL}^{\max}(\tilde{\pi}_{\theta_{old}}(\cdot | s) \| \tilde{\pi}_\theta(\cdot | s))$ . We can get  $M_{\tilde{\pi}_{\theta_{old}}}(\tilde{\pi}_{\theta_{old}}) = \eta(\tilde{\pi}_{\theta_{old}})$ . By maximizing the  $M_{\tilde{\pi}_{\theta_{old}}}(\tilde{\pi}_\theta)$ , we can ensure  $M_{\tilde{\pi}_{\theta_{old}}}(\tilde{\pi}_\theta) \geq M_{\tilde{\pi}_{\theta_{old}}}(\tilde{\pi}_{\theta_{old}}) = \eta(\tilde{\pi}_{\theta_{old}})$ . Given that  $\eta(\tilde{\pi}_\theta) \geq M_{\tilde{\pi}_{\theta_{old}}}(\tilde{\pi}_\theta)$ , we could satisfy the first inequality of Eqn. (4).

By constraining the upper bound of  $\tilde{\pi}_{\theta_{old}}$  to be smaller than  $2\eta(\bar{\pi}) - \eta(\tilde{\pi}_{\theta_{old}})$ , we could guarantee the second inequality of Eqn. (4) holds.

Therefore, combining all these constraints together, we can obtain the following optimization objective:

$$\begin{aligned} \max_{\theta} & L_{\tilde{\pi}_{\theta_{old}}}(\tilde{\pi}_\theta) - C\mathbb{KL}^{\max}(\tilde{\pi}_{\theta_{old}}(\cdot | s) \| \tilde{\pi}_\theta(\cdot | s)) \\ \text{s.t.} & L_{\tilde{\pi}_{\theta_{old}}}(\tilde{\pi}_\theta) + C\mathbb{KL}^{\max}(\tilde{\pi}_{\theta_{old}}(\cdot | s) \| \tilde{\pi}_\theta(\cdot | s)) \leq 2\eta(\bar{\pi}) - \eta(\tilde{\pi}_{\theta_{old}}). \end{aligned} \quad (3)$$

In practice, Schulman *et al.* [11] pointed out that utilizing the penalty coefficient  $C$  may lead to a very small step size. Therefore, we replace the penalty on the maximal KL-divergence with a trust region constraint on an average KL-divergence (*i.e.*,  $\mathbb{E}_{s \sim \rho_{\tilde{\pi}_{\theta_{old}}}}[\mathbb{KL}(\tilde{\pi}_{\theta_{old}}(\cdot | s) \| \tilde{\pi}_\theta(\cdot | s))] \leq \delta$ ) as suggested in [11]. We can further obtain the following objective

$$\begin{aligned}
& \max_{\theta} L_{\tilde{\pi}_{\theta_{old}}}(\tilde{\pi}_{\theta}) \\
& \text{s.t. } L_{\tilde{\pi}_{\theta_{old}}}(\tilde{\pi}_{\theta}) \leq 2\eta(\bar{\pi}) - \eta(\tilde{\pi}_{\theta_{old}}) - \delta, \\
& \mathbb{E}_{s \sim \rho_{\tilde{\pi}_{\theta_{old}}}} [\text{KL}(\tilde{\pi}_{\theta_{old}}(\cdot | s) \| \tilde{\pi}_{\theta}(\cdot | s))] \leq \delta.
\end{aligned} \tag{4}$$

Additionally, we add a sparsity constraint which will only tighten the problem without affecting the monotonicity property and obtain the following optimization objective

$$\begin{aligned}
& \max_{\theta} L_{\tilde{\pi}_{\theta_{old}}}(\tilde{\pi}_{\theta}) \\
& \text{s.t. } \textcircled{1} \mathbb{E}_{a^e \sim \tilde{\pi}_{\theta}} [a^e] \geq c, \\
& \textcircled{2} L_{\tilde{\pi}_{\theta_{old}}}(\tilde{\pi}_{\theta}) \leq 2\eta(\bar{\pi}) - \eta(\tilde{\pi}_{\theta_{old}}) - \delta, \\
& \textcircled{3} \mathbb{E}_{s \sim \rho_{\tilde{\pi}_{\theta_{old}}}} [\text{KL}(\tilde{\pi}_{\theta_{old}}(\cdot | s) \| \tilde{\pi}_{\theta}(\cdot | s))] \leq \delta,
\end{aligned} \tag{5}$$

where  $\mathbb{E}_{a^e \sim \tilde{\pi}_{\theta}} [a^e] \geq c$  constrains the lower bound sparsity for the output of  $\tilde{\pi}_{\theta}$  across all states. By maximizing the local approximation with constraint  $\textcircled{3}$ , we could guarantee that  $L_{\tilde{\pi}_{\theta_{old}}}(\tilde{\pi}_{\theta}) \geq L_{\tilde{\pi}_{\theta_{old}}}(\tilde{\pi}_{\theta_{old}}) = \eta(\tilde{\pi}_{\theta_{old}})$ . Since  $L_{\tilde{\pi}_{\theta_{old}}}(\tilde{\pi}_{\theta})$  is the local approximation of  $\eta(\tilde{\pi}_{\theta})$ , we could further guarantee that  $\eta(\tilde{\pi}_{\theta}) \geq \eta(\tilde{\pi}_{\theta_{old}})$ . Moreover, the constraint  $L_{\tilde{\pi}_{\theta_{old}}}(\tilde{\pi}_{\theta}) \leq 2\eta(\bar{\pi}) - \eta(\tilde{\pi}_{\theta_{old}}) - \delta$  could ensure that the inequality  $\eta(\tilde{\pi}_{\theta}) \leq 2\eta(\bar{\pi}) - \eta(\tilde{\pi}_{\theta_{old}})$  is satisfied. Therefore, a policy  $\tilde{\pi}_{\theta}$  solved from the optimization objective above satisfies Lemma 2 and thus enables the desired monotonicity.

### S3 Derivative from Eqn. (6) to of Eqn. (7)

With respect to  $\theta$ , Eqn. (6) becomes

$$\max_{\theta} (1 - \lambda)L_{\tilde{\pi}_{\theta_{old}}}(\tilde{\pi}_{\theta}) + C_1 \quad \text{s.t. } \mathbb{E}_{s \sim \rho_{\tilde{\pi}_{\theta_{old}}}} [\text{KL}(\tilde{\pi}_{\theta_{old}}(\cdot | s) \| \tilde{\pi}_{\theta}(\cdot | s))] \leq \delta, \quad \mathbb{E}_{a^e \sim \tilde{\pi}_{\theta}} [a^e] \geq c, \tag{6}$$

where  $C_1 = \lambda(2\eta(\bar{\pi}) - \eta(\tilde{\pi}_{\theta_{old}}) - \delta)$  is a constant that can be eliminated during the optimization of  $\theta$ . The KKT condition [1] implies that there exists Lagrange multiplier  $\xi$  (dual solution) such that the set of solutions of the constrained optimization problem Eqn. (6) are equivalent to those of the following relaxed objective:

$$\max_{\theta} (1 - \lambda)L_{\tilde{\pi}_{\theta_{old}}}(\tilde{\pi}_{\theta}) + \xi \mathbb{E}_{a^e \sim \tilde{\pi}_{\theta}} [a^e] \quad \text{s.t. } \mathbb{E}_{s \sim \rho_{\tilde{\pi}_{\theta_{old}}}} [\text{KL}(\tilde{\pi}_{\theta_{old}}(\cdot | s) \| \tilde{\pi}_{\theta}(\cdot | s))] \leq \delta. \tag{7}$$

If  $\lambda < 1$ , the optimization problem is equivalent to

$$\max_{\theta} L_{\tilde{\pi}_{\theta_{old}}}(\tilde{\pi}_{\theta}) + w \mathbb{E}_{a^e \sim \tilde{\pi}_{\theta}} [a^e] \quad \text{s.t. } \mathbb{E}_{s \sim \rho_{\tilde{\pi}_{\theta_{old}}}} [\text{KL}(\tilde{\pi}_{\theta_{old}}(\cdot | s) \| \tilde{\pi}_{\theta}(\cdot | s))] \leq \delta, \tag{8}$$

where  $w = \xi/(1 - \lambda)$ .

The optimization problem can further be transformed as

$$\begin{aligned}
& \max_{\theta} \sum_s \rho_{\tilde{\pi}_{\theta_{old}}}(s) \sum_{a^e} \tilde{\pi}_{\theta}(a^e | s) A_{\tilde{\pi}_{\theta_{old}}}(s, a^e) + w \mathbb{E}_{a^e \sim \tilde{\pi}_{\theta}} [a^e] \\
& \text{s.t. } \mathbb{E}_{s \sim \rho_{\tilde{\pi}_{\theta_{old}}}} [\text{KL}(\tilde{\pi}_{\theta_{old}}(\cdot | s) \| \tilde{\pi}_{\theta}(\cdot | s))] \leq \delta.
\end{aligned} \tag{9}$$

Due to the summation of the new policy  $\tilde{\pi}_{\theta}$ , optimization is still challenging to implement even after transformation. To resolve this issue, we follow the idea from [10]. Specifically, we use importance sampling and substitute it with the summation of the old policy through the Monte Carlo method [14]. Then, in order to reach our ultimate optimization function, we further substitute the trust region constraints with the clipped ratio operation proposed by the Proximal Policy Optimization algorithm (PPO) [11]. Therefore, if  $\lambda < 1$ , we could obtain the final objective to optimize  $\theta$  as

$$\max_{\theta} \mathbb{E} \left[ \min \left( \frac{\tilde{\pi}_{\theta}(a_t^e | s_t)}{\tilde{\pi}_{\theta_{old}}(a_t^e | s_t)} A_{\tilde{\pi}_{\theta_{old}}}, \text{clip} \left( \frac{\tilde{\pi}_{\theta}(a_t^e | s_t)}{\tilde{\pi}_{\theta_{old}}(a_t^e | s_t)}, 1 - \epsilon, 1 + \epsilon \right) A_{\tilde{\pi}_{\theta_{old}}} \right) + w L_t^{\text{MASK}} \right], \tag{10}$$

where  $L_t^{\text{MASK}} = \mathbb{E}_{a_t^e \sim \tilde{\pi}_{\theta}} [a_t^e]$  is added to ensure the sparsity of critical steps.

If  $\lambda > 1$ , the optimization problem is equivalent to

$$\min_{\theta} L_{\tilde{\pi}_{\theta_{old}}}(\tilde{\pi}_{\theta}) - w \mathbb{E}_{a^e \sim \tilde{\pi}_{\theta}} [a^e] \quad \text{s.t.} \quad \mathbb{E}_{s \sim \rho_{\tilde{\pi}_{\theta_{old}}}} [\mathbb{KL}(\tilde{\pi}_{\theta_{old}}(\cdot | s) || \tilde{\pi}_{\theta}(\cdot | s))] \leq \delta. \quad (11)$$

Similar to the analysis above, if  $\lambda > 1$ , the final objective for updating  $\theta$  becomes

$$\max_{\theta} \mathbb{E} \left[ -\min \left( \frac{\tilde{\pi}_{\theta}(a_t^e | s_t)}{\tilde{\pi}_{\theta_{old}}(a_t^e | s_t)} A_{\tilde{\pi}_{\theta_{old}}}, \text{clip} \left( \frac{\tilde{\pi}_{\theta}(a_t^e | s_t)}{\tilde{\pi}_{\theta_{old}}(a_t^e | s_t)}, 1 - \epsilon, 1 + \epsilon \right) A_{\tilde{\pi}_{\theta_{old}}} \right) + w L_t^{\text{MASK}} \right], \quad (12)$$

Putting all these objectives together, we get the final objective for updating  $\theta$  as

$$\max_{\theta} \mathbb{E} \left[ \text{sgn}(1 - \lambda) \min \left( \frac{\tilde{\pi}_{\theta}(a_t^e | s_t)}{\tilde{\pi}_{\theta_{old}}(a_t^e | s_t)} A_{\tilde{\pi}_{\theta_{old}}}, \text{clip} \left( \frac{\tilde{\pi}_{\theta}(a_t^e | s_t)}{\tilde{\pi}_{\theta_{old}}(a_t^e | s_t)}, 1 - \epsilon, 1 + \epsilon \right) A_{\tilde{\pi}_{\theta_{old}}} \right) + w L_t^{\text{MASK}} \right]. \quad (13)$$

## S4 Our Training Algorithm

### S4.1 Algorithm Detail

**Optimizing  $\theta$ .** Recall that the final objective function of  $\theta$  is

$$\max_{\theta} \mathbb{E} \left[ \text{sgn}(1 - \lambda) \min \left( \frac{\tilde{\pi}_{\theta}(a_t^e | s_t)}{\tilde{\pi}_{\theta_{old}}(a_t^e | s_t)} A_{\tilde{\pi}_{\theta_{old}}}, \text{clip} \left( \frac{\tilde{\pi}_{\theta}(a_t^e | s_t)}{\tilde{\pi}_{\theta_{old}}(a_t^e | s_t)}, 1 - \epsilon, 1 + \epsilon \right) A_{\tilde{\pi}_{\theta_{old}}} \right) + w L_t^{\text{MASK}} \right], \quad (14)$$

where  $A_{\tilde{\pi}_{\theta_{old}}} = A_{\tilde{\pi}_{\theta_{old}}}(s_t, a_t^e)$  and  $L_t^{\text{MASK}}(\theta) = \mathbb{E}_{a_t^e \sim \tilde{\pi}_{\theta}} [a_t^e]$ .

Note that the output of `StateMask`  $a_t^e$  is sampled from a categorical distribution over all actions (*i.e.*, 0 or 1). However, as stated in [4], the categorical variable  $a_t^e$  is not capable of backpropagating through samples. Note that  $\mathbb{E}_{a_t^e \sim \tilde{\pi}_{\theta}} [a_t^e] = \mathbb{E}_{s_t \sim \rho_{\tilde{\pi}_{\theta}}} [\mathbb{E}_{a_t^e \sim \tilde{\pi}_{\theta}(\cdot | s)} [a_t^e]] = \mathbb{E}_{s_t \sim \rho_{\tilde{\pi}_{\theta}}} [Pr(a_t^e = 1)]$  and  $Pr(a_t^e = 1)$  is differentiable. Therefore, we replace  $\mathbb{E}_{a_t^e \sim \tilde{\pi}_{\theta}} [a_t^e]$  with  $\mathbb{E}_{s_t \sim \rho_{\tilde{\pi}_{\theta}}} [Pr(a_t^e = 1)]$  in practice.

When estimating  $A_{\tilde{\pi}_{\theta_{old}}}$ , we adopt the same estimation formula as PPO[11]

$$\begin{aligned} \hat{A}_{\tilde{\pi}_{\theta_{old}}} &= \delta_t + (\gamma \zeta) \delta_{t+1} + \dots + \dots + (\gamma \zeta)^{T-t+1} \delta_{T-1} \\ \text{where } \delta_t &= r_t + \gamma V(s_{t+1}) - V(s_t) \end{aligned} \quad (15)$$

Therefore, during the training process, in addition to updating the actor by solving  $\theta$  in Eqn. (14), we also have to update the state-value function  $V(s)$  by the Temporal-Difference (TD) method [13] for better estimating the advantage.

**Optimizing  $\lambda$ .** And recall that the objective function of  $\lambda$  is

$$\min_{\lambda \geq 0} \lambda \left( 2\eta(\tilde{\pi}) - \eta(\tilde{\pi}_{\theta_{old}}) - \delta - L_{\tilde{\pi}_{\theta_{old}}}(\tilde{\pi}_{\theta}) \right). \quad (16)$$

where  $L_{\tilde{\pi}_{\theta_{old}}}(\tilde{\pi}_{\theta}) = \sum_s \rho_{\tilde{\pi}_{\theta_{old}}}(s) \sum_{a^e} \tilde{\pi}_{\theta}(a^e | s) A_{\tilde{\pi}_{\theta_{old}}}(s, a^e)$ .

In practice,  $\eta(\tilde{\pi}_{\theta_{old}})$  and  $\eta(\tilde{\pi})$  can be approximated via Monte Carlo method [7].  $\eta(\tilde{\pi})$  can be estimated in advance, *i.e.*, running the game with the agent’s policy  $\tilde{\pi}$  500 times and calculating the average expected discounted reward as follows

$$\eta(\tilde{\pi}) = \mathbb{E}_{s_0, a_0, \dots \sim \tilde{\pi}} \left[ \sum_{t=0}^{\infty} \gamma^t r(s_t) \right], \quad (17)$$

$\eta(\pi_{\theta_{old}})$  can be estimated using a similar formula in parallel with the collecting trajectories of old policy  $\pi_{\theta_{old}}$  while solving  $\theta$  with our training algorithm.

Nevertheless, the optimization objective remains challenging to solve because of the summation in  $L_{\tilde{\pi}_{\theta_{old}}}(\tilde{\pi}_{\theta})$  involving the new policy  $\tilde{\pi}_{\theta}$ . To address this issue, we utilize importance sampling and substitute the summation over the new policy  $\tilde{\pi}_{\theta}$  with a summation over the old policy  $\tilde{\pi}_{\theta_{old}}$ , which can be computed using the Monte Carlo method [7]. Mathematically,  $L_{\tilde{\pi}_{\theta_{old}}}(\tilde{\pi}_{\theta})$  can be estimated by  $\frac{\tilde{\pi}_{\theta}(a^e | s)}{\tilde{\pi}_{\theta_{old}}(a^e | s)} A_{\tilde{\pi}_{\theta_{old}}}(s, a^e)$ , which has already been computed in Eqn. (14) when updating  $\theta$ .

---

**Algorithm 1** The training algorithm of mask net.

---

**Input:** Target agent’s policy  $\bar{\pi}$   
**Output:** Mask net policy  $\tilde{\pi}$   
**Initialization:** Initialize the weights  $\theta$  for the mask net  $\tilde{\pi}$ , Lagrange multiplier  $\lambda = 0$   
Estimate the  $\eta(\bar{\pi})$  in advance by Eqn. (17)  
**for**  $iteration = 1, 2, \dots$  **do**  
     $s \leftarrow s_0$   
     $\mathcal{D} \leftarrow \emptyset$   
    **for**  $t = 1, 2, \dots, T$  **do**  
         $a_t^e \leftarrow$  sample from  $\tilde{\pi}_{\theta_{old}}(\cdot|s)$   
         $a_t \leftarrow$  sample from  $\bar{\pi}(\cdot|s)$   
        Compute actual taken action  $a \leftarrow a_t \odot a_t^e$   
        Obtain current step reward  $r_t$ , next state  $s'$  from the environment given action  $a$   
         $\mathcal{D} \leftarrow \mathcal{D} \cup (s, a_t^e, r_t, s')$   
         $s \leftarrow s'$   
    **end for**  
    Compute estimates for  $A_{\tilde{\pi}_{\theta_{old}}}(s_t, a_t^e)$  using samples in  $\mathcal{D}$  by Eqn. (15)  
    Solve  $\theta$  using the trajectory samples in  $\mathcal{D}$  by Eqn. (14) and update  $\theta_{old} \leftarrow \theta$   
    Estimate the  $\eta(\tilde{\pi})$  using the trajectory samples in  $\mathcal{D}$  by Eqn. (17)  
    Solve  $\lambda$  by Eqn. (16) and update  $\lambda_{old} \leftarrow \lambda$   
**end for**

---

**Extensive-form Games.** Regarding extensive-form games, we train a state mask for the target agent while keeping all the agents’ policies fixed. In this way, we could transform the extensive-form games into single-player normal-form games (*i.e.*, we treat all of the agents’ actions as part of the environment). However, the game may not end with the target agent, and the target agent will not receive the game reward in this case. To address this problem, we automatically overwrite the target agent’s final reward with the final game result.

Based on what we have discussed above, we present the full algorithm in Algorithm 1.

## S4.2 Implementation and Hyperparameters

We implement our training algorithm using PyTorch [9] and additionally discuss the hyperparameter setting of our training algorithm. The common hyperparameter setting is as follows. Regarding the clipping parameter  $\epsilon$  in Eqn. (14), we set it as 0.2. As for the advantage estimation in Eqn. (15), we set  $\gamma = 0.99$  and  $\zeta = 0.95$ . Moreover, we provide the game-specific hyperparameter choices in Table 1. Regarding the policy network of `StateMask`, we utilize a widely used network structure, commonly employed to train Deep Reinforcement Learning (DRL) agents for each game. Specifically, we use Convolutional Neural Network (CNN) for the Pong game and Residual Network (ResNet) for the Connect 4 game since these two games’ input observation contains spatial information and are relatively complicated. For other games, we use either Long Short-Term Memory (LSTM) or Multi-Layer Perceptron (MLP) network, which depends on the input type of the observation and the game’s complexity. We use two separate networks with the same backbone architecture for the policy and value networks. The output dimension of the policy network and value network are 2 and 1, respectively. As for the learning rate setting, we refer to other work of training a reinforcement learning agent in these games [6, 2]. Moreover, our method introduces an extra hyperparameter –  $w$  (To encourage the mask network to blind the target agent at some states, we add a sparsity constraint on the number of mask actions). We search the  $w$  in  $\{0, 1e-5, 1e-4, 1e-3, 1e-2\}$  and report the sensitivity experiment results in Supplement S5.3.

Table 1: Training hyperparameter settings of our method. The numbers in the bracket after "CNN" represent the number of kernels in each layer. The numbers in the bracket after "MLP" are the hidden dimensions.  $512 \times 10$  represents 10-layer MLP with hidden size 512.

Games	$w$	Learning rate	Optimizer	StateMask backbone	Batch Size	Num. of Training Steps
Pong	1e-4	1e-5	Adam	CNN(16, 32)	32	2e+4
You-Shall-Not-Pass	0	3e-4	Adam	MLP(256, 256)	2048	2e+7
Kick-And-Defend	0	3e-4	Adam	LSTM(512, 256)	2048	2e+7
CartPole	0	1e-3	Adam	MLP(256, 256)	5	8e+2
Pendulum	0	1e-3	Adam	MLP(256, 256)	5	8e+2
StarCraft II	0	1e-6	Adam	MLP(128,128,128)	32	8e+7
Connect 4	1e-3	1e-3	Adam	ResNet-128	1024	4e+5
Tic-Tac-Toe	1e-5	1e-2	Adam	MLP(128, 128)	128	2e+4
Breakthrough	1e-3	1e-3	Adam	MLP(512 $\times$ 10)	1024	2e+6
DouDizhu	1e-3	3e-4	Adam	MLP(512 $\times$ 10)	42	8e+5

## S5 Details of Evaluation

### S5.1 Other Implementation Details

**Baseline Implementations.** Regarding baseline approaches, we use the code released by the authors or implement our own version if the authors don't release the code. Specifically, as for EDGE, we use their released open-sourced code from <https://github.com/Henrygwb/edge>. For the Value-max and the LazyMDP method, we assume that we have access to the target agent's value function and implement them based on the description of the original method<sup>1</sup>.

**Fidelity Tests and Metrics.** As mentioned in Section 4.2, we adopt the experiment design in EDGE [3] to access the accuracy of the explanation. Specifically, the fidelity test first gathers  $N$  (*i.e.*,  $N = 500$  in our setting) trajectories. Each explanation method generates the importance score of each state accordingly without altering the agent's action. For each trajectory, we identify and record the length  $l$  of the longest continuous sequence within the top- $K$  most critical time steps. Following this, we replay the sequence of actions from the original trajectory up to the start of this identified sequence. From this point onwards, we replace the original actions with randomly selected actions for the next  $l$  steps. Once the action substitution is completed, we present the newly reached state to the target agent at the end of the selected time steps. From this point forward, the agent operates according to the actions suggested by its policy network until the conclusion of the game. The reward difference before and after action replacement is denoted as  $d$ . The fidelity score is defined as  $\log(p_d) - \log(p_l)$  where  $p_d = |d|/d_{max}$  is the absolute reward difference divided by the maximum possible reward difference and  $p_l = l/L$  is the length of the longest sequence normalized by the original trajectory length  $L$ . Note that in the original definition of the fidelity score [3], a lower score implies a higher level of fidelity. However, for ease of presentation, we have introduced a negative sign to the fidelity score, such that a higher score indicates superior fidelity.

### S5.2 Experiment Setup

**Game Introduction and Target Agents.** To assist in determining whether our explanation aligns with human perception, we briefly introduce each game below.

- **Pong** is a two-dimensional sports game that simulates table tennis as Figure 1 shows. The RL agent controls the right paddle while a decent AI from the Atari game environment controls the left paddle. The RL agent observes itself, the opponent, and the position of the ball before deciding whether to move the paddle up, down, or take no action. In each round, the RL agent wins the game and collects a +1 reward if the opponent fails to return the ball; the agent loses the game and collects a 0 reward if it misses the ball. To facilitate the evaluation, we terminate the game at the end of each round.

<sup>1</sup>For the Value-max, since it is relatively easy to implement, we only need to extract the state value from the value function. As to the LazyMDP, we contacted the author and implemented the explainer based on the author's response.

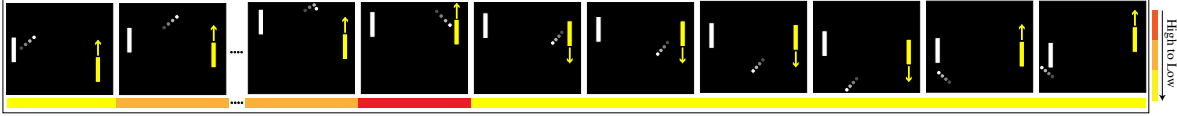


Figure 1: Visualization of the identified critical time steps in Pong game. The DRL agent controls the yellow paddle and a non-RL rule-based opponent controls the white paddle.

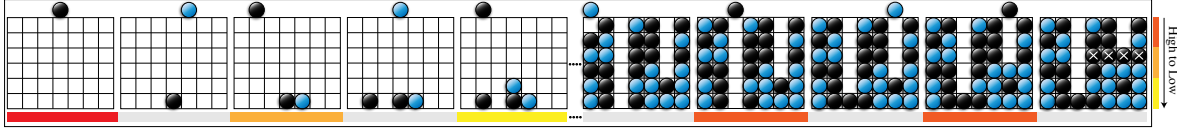


Figure 2: Visualization of the identified critical steps in the Connect 4 game. The black player is our explanation target player. Note that the states where the blue player takes actions are marked with a gray bar.

- **You-Shall-Not-Pass** is a two-party competitive game as Figure 6 shows. Two humanoid robots face each other at the beginning of the game. The red robot then starts running towards the finish line (indicated by the red line), while the blue robot is tasked with preventing the runner from achieving its goal. In our evaluation, the red robot wins the game if it can get across the finish line. Otherwise, the blue blocker wins. The red robot gets the reward  $+1$  once it wins the game and  $-1$  when it loses the game
- **Kick-And-Defend** is a two-party competitive game as Figure 7 shows. Two humanoid robots compete in a soccer penalty shootout. The placements of kicker, defender, and ball are all chosen at random. If the ball falls between the goalposts, the kicker wins; otherwise, the defender wins. The reward is  $+1$  for the kicker to win the game and  $-1$  when the kicker loses.
- **CartPole** is one of OpenAI’s open-source environments as Figure 8 shows. The “cartpole” agent is a reverse pendulum in which a “cart” attempts to vertically balance a “pole” with a slight angle adjustment. The only forces that can be used are represented by  $+1$  and  $-1$ , corresponding to a left and right movement, respectively. The episode ends if the cart moves more than 2.4 units away from the center or if the angle deviates from vertical by 15 degrees. For each timestamp that the episode hasn’t ended, the reward is increased by one. The maximum reward available is 500.
- **Pendulum** simulates the inverted pendulum swingup problem as Figure 9 shows. The pendulum starts in a random position, and the goal is to swing it up and keep it upright. The pendulum angle is represented by  $\theta$ , which starts at random from  $-\pi$  to  $\pi$ . The default reward function is based on the angle  $\theta$  and the agent’s action  $a$ . To maximize rewards, the agent must keep the angle  $\theta$  at zero, rotate at the slowest possible speed, and exert the least amount of effort.
- **StarCraft II** is a popular real-time strategy game as Figure 10 shows. The player controls an army to defeat the opponent’s base by collecting resources and building units. The player’s observation is the minimap and the screen. The minimap shows the entire map, while the screen shows the player’s view. The player can take actions such as selecting units, and issuing commands to the units. The player wins if the opponent’s base is destroyed, and the game ends if the player’s base is destroyed. The winning, and losing outcomes of the player correspond to  $+1$  and  $-1$  rewards, respectively.
- **Connect 4** uses a  $6 \times 7$  grid as Figure 2 shows. Players take turns dropping tokens into the grid. The tokens land straight down, taking up the lowest available space in the column. The player wins if any four of the tokens are in a row horizontally, vertically, or diagonally. The game could also end in a draw if the grid is full while no player wins. The winning, draw, and losing outcomes of the player correspond to  $+1$ ,  $0$ , and  $-1$  rewards, respectively.
- **Tic-Tac-Toe** uses a  $3 \times 3$  grid as Figure 11 shows. Two players iteratively place a symbol on an available position. The player wins if any three of the symbols are in a row horizontally, vertically, or

Table 2: Game information with the target agents to explain. "Discrete(X)" refers to X discrete actions available to choose from. "Vector(X)" refers to X-dimension continuous action space.

Games	Observation shape	Action space	Reward range	Target agent
Pong	(84,84)	Discrete(6)	0,1	Pong agent
You-Shall-Not-Pass	(380)	Vector(17)	-1,1	Runner
Kick-and-Defend	(380)	Vector(17)	-1,1	Kicker
CartPole	(4)	Discrete(2)	[0,500]	CartPole agent
Pendulum	(3)	Vector(1)	[-1200,0]	Pendulum agent
StarCraft II	(919)	Discrete (165)	-1,1	StarCraft II bot
Connect 4	(3,6,7)	Discrete(7)	-1,0,1	First player
Tic-Tac-Toe	(3,3,3)	Discrete(9)	-1,0,1	First player
Breakthrough	(8,8)	Discrete(3)	-1,1	First player
DouDizhu	(23, 54)	Discrete(Undertermined)	0,1	Landlord

diagonally. The game could also end in a draw if the grid is full while no player wins. The winning, draw, and losing outcomes of the player correspond to +1, 0, and -1 rewards, respectively.

- **Breakthrough** uses a  $8 \times 8$  grid as Figure 12 shows. Two players iteratively move one piece. If the target square is unoccupied, a piece may advance one space either straight forward or diagonally. Only if the square containing the opponent’s piece is one step diagonally forward may a piece move into and replace it. The winner is the first player to reach the opponent’s home row. A player loses if all of his pieces are taken. A draw is impossible in the Breakthrough game. The winning and losing outcomes of the player correspond to +1 and -1 rewards, respectively.
- **DouDizhu** is a three-party card game as Figure 13 shows. Players begin the game by putting in bids for the “landlord”. The other two players will act as “peasants”. Being the first player to run out of cards is the game’s goal. By removing all of their cards first, the landlord prevails. If one of the peasants removes all of their cards first, the peasants win. The winning and losing outcomes of the landlord correspond to +1 and -1 rewards, respectively.

We also list some basic information (*e.g.*, observation shape, action space, and reward range) about these selected games in Table 2. Besides, we clarify the target agent to explain in Table 2 as well (*i.e.*, except for OpenAI gym and the Atari games, all the other games are multi-agent games, and we intend to one specific party). For the Pong game, we train an agent based on the PPO algorithm to achieve a relatively high reward (*i.e.*, 0.906 in our setting). Regarding two MuJoCo games, we target to explain the runner in You-Shall-Not-Pass and the kicker in Kick-And-Defend. The DRL models of the target agents in the two MuJoCo games are downloaded from <https://github.com/openai/multiagent-competition/tree/master/agent-zoo>. As for OpenAI’s CartPole and Pendulum games, we adopt well-trained agents from the stable-baselines3 model zoo: <https://github.com/DLR-RM/r1-baselines3-zoo>. With respect to Connect 4, Breakthrough, and Tic-Tac-Toe, we explain the first player and utilize example codes in OpenSpiel for training RL agents based on the AlphaZero algorithm [12]. The maximum simulation times for the Monte Carlo Tree Search in Connect 4, Breakthrough, and Tic-Tac-Toe are 300, 300, and 20, respectively. Concerning DouDizhu, we target at explaining the landlord and adopt the models trained by DouZero [16], which can be downloaded from <https://github.com/kwai/DouZero>. When it comes to StarCraft II, we use the built-in bot with difficulty A from PySC2: <https://github.com/deepmind/pysc2>.

**Computational Resources.** In our experiment, we use a server with 2 AMD EPYC 7702 64-Core CPU Processors and 4 NVIDIA RTX A6000 GPUs to train and evaluate our method.

### S5.3 Additional Evaluation Results

First, we demonstrate that our design could achieve the monotonicity property by showing the training curves of all games. Second, we provide the agent’s performance and StateMask’s performance on all games and show the relative value errors across all games. Last, we compare the fidelity scores of our

Table 3: **Results of reward gap in all games.** Each experiment contains 500 runs. We repeat all experiments three times and report the mean and standard deviation of the discounted total rewards in the table below.

Games	Agent Performance	Relative Errors (%)	Games	Agent Performance	Relative Errors (%)
Pong	0.20 (0.00)	0.89 (0.03)	StarCraft II	0.11 (0.00)	0.40 (0.01)
You-Shall-Not-Pass	-0.13 (0.01)	2.58 (0.12)	Connect 4	0.91 (0.01)	2.09 (0.12)
Kick-And-Defend	0.13 (0.01)	7.78 (0.20)	Tic-Tac-Toe	0.76 (0.02)	6.43 (0.08)
CartPole	99.34 (0.00)	0.00 (0.00)	DouDizhu	0.40 (0.02)	14.98 (0.21)
Pendulum	-144.16 (10.26)	5.56 (0.33)	Breakthrough	0.98 (0.00)	11.02 (0.16)

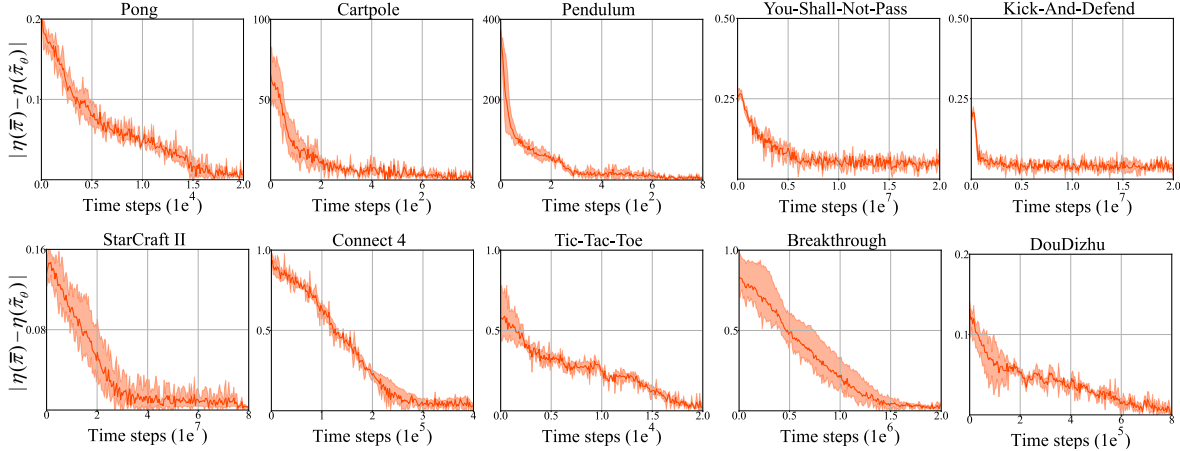


Figure 3: The absolute policy value difference between the masked agent trained by **StateMask** and the target agent. Note that the darker solid lines represent the average absolute policy value difference across 3 random seeds. The lighter shadow indicates the corresponding variations between the maximal and minimal absolute policy value difference.

method with three baseline methods on additional five games, *i.e.*, Kick-And-Defend in MuJoCo games, OpenAI’s Cartpole and Pendulum, Breakthrough and Tic-Tac-Toe in Openspiel.

**Monotonicity Property.** Figure 3 shows the trend of  $|\eta(\bar{\pi}) - \eta(\bar{\pi}_\theta)|$  (*i.e.*, the absolute policy value difference) during the training processes of all games. As we can observe, the absolute policy value difference monotonically decreases until it converges when the training step increases. Combined with Section 3, it demonstrates that our design could guarantee the monotonicity property both theoretically and empirically.

**Agent Performance.** To evaluate the agent’s performance before and after applying the explanation network, we run 500 tests and record the mean and standard deviation of the discounted total reward in Table 3. We can observe that the agent before and after blinding achieves similar performance when running 500 episode tests. It confirms that our proposed method could achieve the objective in Section 3 (*i.e.*, perturbing the actions in the identified non-important time steps will not impact the expected total reward of the target agent).

**Fidelity.** Section 4 shows the fidelity score comparison between our method and three baseline methods on Pong, You-Shall-Not-Pass, Connect 4, DouDizhu, and StarCraft II. Here, we additionally evaluate the fidelity of our method and three baseline methods on the remaining five games. Figure 4 shows the fidelity score comparison across all four methods. Combined with Figure 3 in Section 4, **StateMask** consistently achieves the highest fidelity score among all games, implying our method’s high fidelity.

**Sensitivity.** To show the insensitivity of our proposed method **StateMask**, we vary the hyperparameter  $w$  from  $\{0, 1e-5, 1e-4, 1e-3, 1e-2\}$  and train the state mask accordingly. Figure 5 (a) and (b) shows the fidelity scores and mask ratios of our method in Pong and You-Shall-Not-Pass games under different  $w$  settings. We can observe that through the hyperparameter  $w$  differs, the fidelity scores do not vary too much. It confirms that our method is insensitive to hyperparameter choice. Moreover, adding a sparsity constraint can increase the mask ratio which can help filter out those non-important time steps.

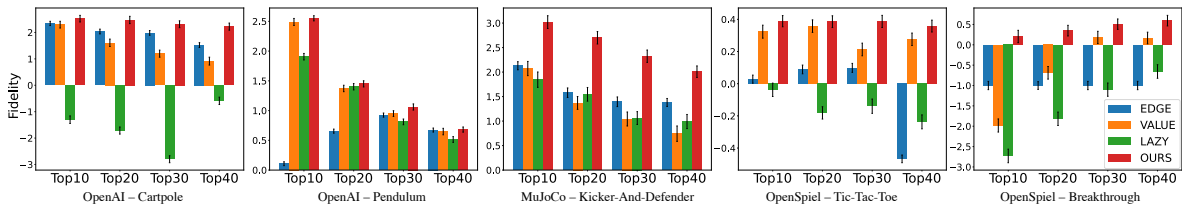


Figure 4: Fidelity scores for interpretations generated by three baseline methods and our proposed explanation method. Note that the definition of the fidelity score can be found in Section 4.2. A higher score implies higher fidelity.

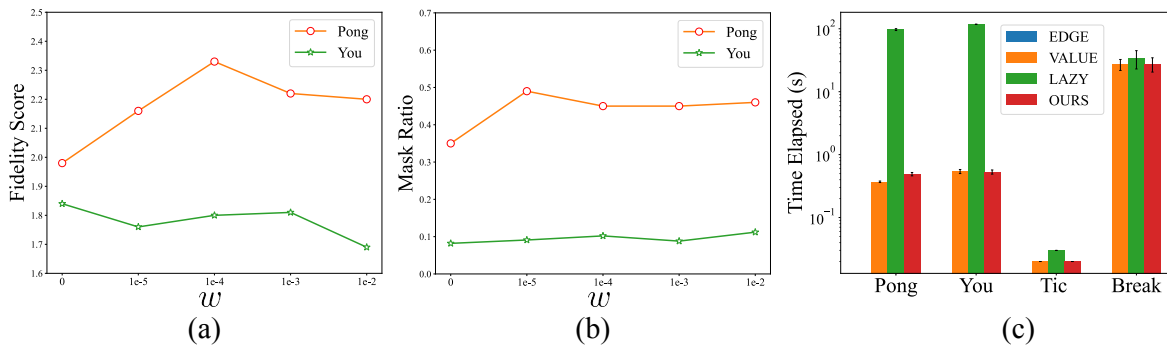


Figure 5: Sensitivity and efficiency results. In the left and middle figures, we show the sensitivity results by varying the hyperparameter  $w$  in Pong and You-Should-Not-Pass games. In the right figure, we report the mean and standard deviation of the explanation time per trajectory in four games: Pong, You-Should-Not-Pass, Tic-Tac-Toe, and Breakthrough.

**Efficiency.** To demonstrate our method’s efficiency, we also record the average explanation time per trajectory in two normal-form games and two extensive-form games. Figure 5 (c) shows the explanation time of each method in four games. Here, EDGE is a global explanation method whose explanation time is negligible while the other three are local explanation methods. Regarding local explanation methods, our proposed method `StateMask` has similar time efficiency with the Value-max method whereas LazyMDP is much slower. The reason is that the target agents in these four games cannot provide the Q value function directly, and thus we need extra computation time to approximate Q values for deriving explanations in LazyMDP.

## S6 Additional Visualization Results

**You-Should-Not-Pass.** In Figure 6, we visualize one episode of the You-Should-Not-Pass game. Our explainer pinpoints the time steps when the red robot escapes the blue robot as the most important ones. The reason is that the DRL agent should be careful not to get knocked down by the opponent at this moment. Otherwise, the agent will lose the balance and fall to the ground, and eventually lose the game. When the two robots are far away from each other or the blue robot is already down on the ground, the states are less important.

**Kick-And-Defend.** We provide one case study for the Kick-And-Defend game in Figure 7. Our explanation method explains that the most important time steps in this game are when the blue robot is shooting. The agent should choose the proper direction and power to kick the ball to the goal at these critical time steps. Otherwise, it will be difficult for the agent to score. When the ball is flying toward the goal, the actions of the DRL agent have no impact on the final result. Therefore, these time steps are less important.

**CartPole.** For the CartPole game, we show an example in Figure 8. When the angle of the pole is large (no matter if it is clockwise or counterclockwise), the cart should accelerate toward the center to correct the angle, otherwise the pole will fall. `StateMask` treats these time steps as critical ones. When

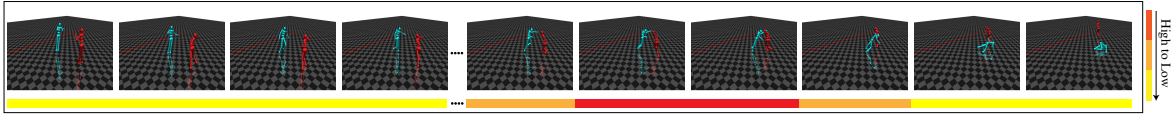


Figure 6: Visualization of the identified critical time steps in You-Sharp-Not-Pass game. The DRL agent controls the red humanoid robot and the opponent controls the blue one. While the blue humanoid bot is trying to block the red one from reaching the goal, the red one is trying to get across the red line.

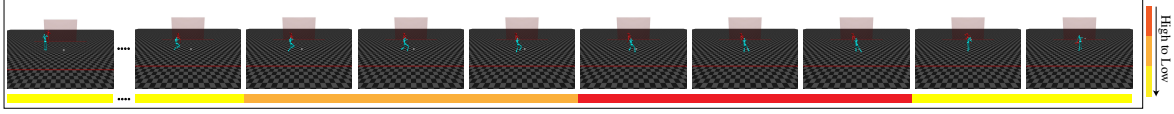


Figure 7: Visualization of the identified critical time steps in Kick-And-Defend game. The DRL agent controls the blue humanoid robot to kick the ball and the opponent controls the red one to defend the goal.



Figure 8: Visualization of the identified critical time steps in Cartpole game. The DRL agent controls the cart to move left or right to keep the pole stand (within a certain angle) as long as possible.

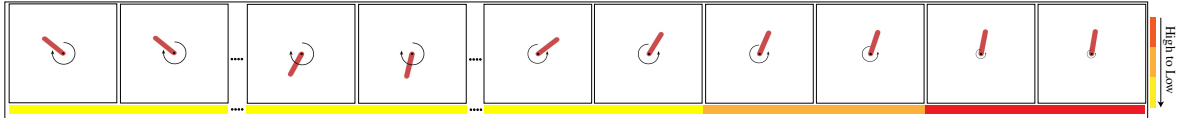


Figure 9: Visualization of the identified critical time steps in Pendulum game. The DRL agent controls the torque applied on the free end of the pendulum to swing it into an upright position, with its center of gravity right above the fixed point.

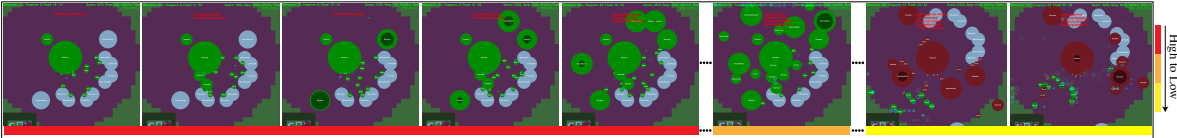


Figure 10: Visualization of the identified critical steps in StarCraft II. The green zerg player is the target agent and the red one is the opponent. The big circles represent the buildings while the small circles represent the units. In the first three steps, the agent collects the minerals and vespene gas. In the next three steps in this episode, the agent builds some structures. In the last two steps, the small circles representing the zerglings and roaches of the target agent are attacking the enemy base.

the angle of the pole is small, the cart needs to stabilize the angle, and `StateMask` treats these time steps as less important ones. This is reasonable since the pole is still within a safe angle range at these time steps.

**Pendulum.** In the Pendulum game, we show one case study in Figure 9. The pendulum starts in a random position and the agent tries to swing it into an upright position. `StateMask` pinpoints the time steps when the pendulum is close to the upright position as the most important ones. The agent should carefully apply the torque at these time steps to make the pendulum upright with zero velocity. When the angle of the pendulum is large, `StateMask` treats these time steps as non-critical ones.

**StarCraft II.** In the StarCraft II game, the DRL agent controls a Zerg player to defeat the opponent Zerg player by collecting resources and building a Zerg army. Figure 10 shows one roach rush game where the DRL agent wins. `StateMask` identifies the first few steps as critical ones, including producing the drones and overlords, as well as building the spawning pool, extractors, and roach warren. These steps are reasonable and will also be deemed as important by human analysis since the successful execution of the build orders in the early stage is one key to winning the game. Also, `StateMask`

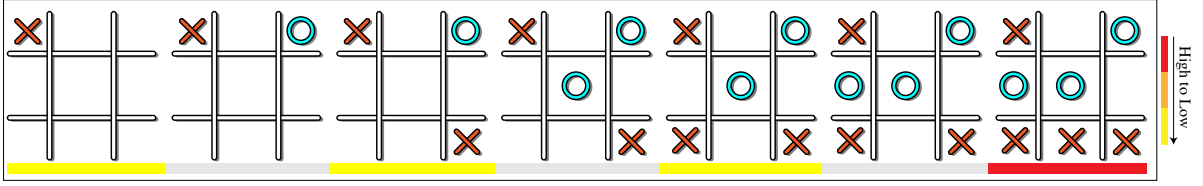


Figure 11: Visualization of the identified critical time steps in the Tic-Tac-Toe game. The DRL agent places the X mark and the opponent places the O alternately in one of the nine spaces in the grid. The states where the O mark is placed are colored in gray.

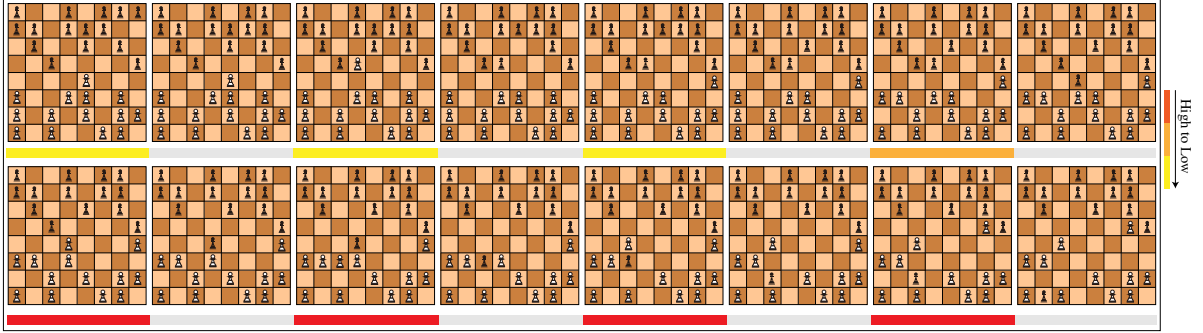


Figure 12: Visualization of the identified critical time steps in Breakthrough game. The DRL agent plays as the black player and the opponent plays as the white one. They play alternatively, with each player moving one piece per turn.

treats the last few steps as non-important steps. This is because the opponent’s army has already been crashed by the roach rush, and without the army’s protection, it is just a matter of time before the agent destroys the opponent’s base to win the game. Because of the automatic attack mechanism in Starcraft II, even if the DRL agent does not take any action, the roaches will destroy all the opponent’s buildings eventually.

**Tic-Tac-Toe.** In the Tic-Tac-Toe game, we show one episode to analyze the explanation of our method in Figure 11. Our explainer only selects the last time step as the critical one since this move seals a win for the DRL agent. If the agent chooses the wrong move at this time step, the opponent will win the game.

**Breakthrough.** Finally, we visualize one episode of the Breakthrough game in Figure 12. Our explainer pinpoints the last four time steps in this episode as the most important. By analyzing the strategy of the agent, we could find that the agent sacrifices one piece to make sure another piece can reach the opponent’s side in the last four time steps. If the agent does not take such a strategy, the game will last for a longer time and the agent may lose the game eventually.

**DouDizhu.** In DouDizhu, a landlord (our target agent) competes with two cooperative peasants to be the first to run out of cards. Figure 14 shows one critical step identified by `StateMask`. At this step, the landlord chooses to play eight cards, *i.e.*, Quad with Pairs. This move enables the landlord to play most low-rank cards and win the right to play first in the next round (no peasant has larger combinations than this one). If these cards are not played together, it is hard for the landlord to play them separately because the Quad and two Pairs are relatively small and cannot help the landlord to get the right to continue playing first.

We also give the winning trajectory for the DouDizhu game in Figure 13. Our explainer pinpoints two critical time steps in this episode. The first one is when the landlord plays **2**. Since **Red Joker** in hand is the largest solo that can beat any other solo, the landlord can ensure the right to play cards in the next round. The second one is when the landlord plays **Trio with Solo** to empty his’s hand. If the landlord plays **Trio** or **Pair** separately, the peasant will have a chance to win the game. Therefore, the two selected time steps are critical to the final result.

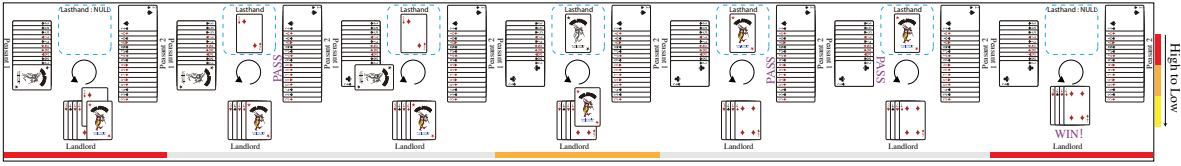


Figure 13: Visualization of the identified critical time steps in the DouDizhu game. The DRL agent plays the role of the landlord and two cooperative opponents play the role of the peasants. The landlord’s goal is to win the game by emptying his hand, and vice versa. The states where the peasants take actions are marked with a gray bar.

## S7 Additional Results of Attacks

In this section, we provide the results of launching adversarial attacks under the guidance of explanation when varying the attack ratio between 10% and 30% in Table 4. First, we can observe that when the threshold increases, the victim agent’s performance drops. Second, with the same threshold setting, the adversarial attack under the guidance of our explanation method is the most powerful one. These results confirm the conclusion that our proposed explanation method has the highest fidelity.

## S8 Additional Results of Policy Patching

**Advantage of Our Patching Method.** In this experiment, we run the patching method proposed in EDGE [3] on two MuJoCo games. At a high level, this method first replays the losing trajectory until the start of the critical steps and does random explorations at the critical steps in order to find a winning strategy. The actions together with the corresponding critical steps in the winning strategy are recorded. Then, it forms a look-up table with these collected state-action pairs and uses the look-up table to remediate the original policy. We follow the setting in EDGE and run 500 tests to obtain the target agents’ winning rate change before and after patching. Table 5 shows the results of EDGE’s patching method. Although the agents’ performances have some improvements after utilizing the EDGE’s patching method, the improvements are overall marginal. Together with the results in Table 1 in Section 5 and Table 6, we can safely conclude the superiority of our proposed patching method over EDGE’s patching method after retraining. The reason may be that EDGE uses a hard rule (*i.e.*, look-up table) to patch the agents’ policy, and the quality of the look-up table has a great influence on the patched agents’ final performance. In contrast, our patching method does not require a fixed look-up table to store the correct actions corresponding to critical states while encouraging the DRL agent to do more exploration at critical time steps and update the neural network parameters accordingly.

**Patching Results on Other Games.** Table 6 provides the agent performance improvement results after retraining under the guidance of our explanation method and the three baselines in Pendulum, Kick-And-Defend, and Tic-Tac-Toe. Using our proposed retraining method under the guidance of explanation, the performance of the reinforcement learning agent generally increases. More importantly, retraining based on our explanation achieves the best performance.

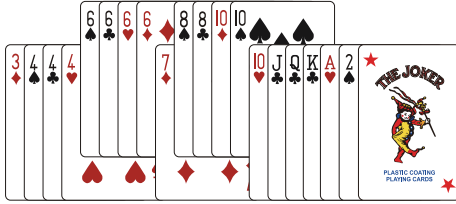


Figure 14: One critical step in the DouDizhu game: The target agent (landlord) plays the Quad with Pairs to ensure that peasants cannot beat this hand.

Table 4: Winning rate drop of varying attack ratios in all games. Each experiment contains 500 runs. We repeat all experiments three times and report the average rewards with the corresponding standard deviations in the table below.

Games	Attack ratio	EDGE	Value-max	LazyMDP	Ours
Pong	10%	-63.04 (3.44)	-0.40 (0.40)	-36.17 (1.15)	<b>-84.90 (1.40)</b>
	20%	-65.73 (0.81)	-7.06 (8.81)	-57.00 (0.92)	<b>-85.53 (0.75)</b>
	30%	-71.07 (1.36)	-70.13 (0.64)	-62.63 (1.63)	<b>-86.90 (0.76)</b>
You-Shall-Not-Pass	10%	-2.64 (0.60)	-14.80 (3.20)	-28.87 (1.21)	<b>-35.93 (1.81)</b>
	20%	-6.87 (0.61)	-55.13 (4.27)	-50.63 (0.80)	<b>-61.67 (0.12)</b>
	30%	-11.68 (1.70)	-61.93 (0.12)	-61.87 (0.23)	<b>-61.93 (0.12)</b>
Kick-And-Defend	10%	-10.46 (0.97)	-24.57 (1.86)	-28.33 (1.76)	<b>-28.37 (1.10)</b>
	20%	-28.51 (0.72)	-64.23 (1.63)	-60.43 (1.33)	<b>-68.63 (1.17)</b>
	30%	-37.25 (1.03)	-74.30 (0.40)	-73.57 (1.53)	<b>-74.10 (0.80)</b>
CartPole	10%	-78.98 (4.61)	-4.85 (6.64)	-0.50 (0.51)	<b>-127.81 (13.82)</b>
	20%	-153.21 (11.87)	-20.96 (6.21)	-13.92 (6.42)	<b>-198.06 (24.21)</b>
	30%	-237.03 (5.30)	-72.99 (7.98)	-56.71 (2.79)	<b>-332.05 (16.33)</b>
Pendulum	10%	-58.84 (2.79)	-255.80 (15.92)	-135.23 (1.51)	<b>-570.77 (1.13)</b>
	20%	-129.37 (1.86)	-432.15 (43.03)	-241.20 (0.95)	<b>-707.69 (0.74)</b>
	30%	-201.39 (3.31)	-563.63 (15.16)	-372.88 (4.21)	<b>-796.07 (12.07)</b>
StarCraft II	10%	-70.00 (14.18)	-77.33 (5.69)	-72.00 (13.53)	<b>-83.00 (7.21)</b>
	20%	-93.33 (4.73)	-93.00 (3.61)	-93.00 (4.58)	<b>-94.00 (3.00)</b>
	30%	-97.00 (0.00)	-97.00 (0.00)	-97.00 (0.00)	<b>-97.00 (0.00)</b>
Connect 4	10%	-33.33 (1.56)	-26.30 (1.44)	-22.57 (1.40)	<b>-35.37 (3.00)</b>
	20%	-56.73 (2.30)	-67.57 (1.57)	-53.83 (0.81)	<b>-71.90 (1.44)</b>
	30%	-76.23 (1.94)	-82.70 (0.80)	-69.83 (1.17)	<b>-85.50 (0.72)</b>
Tic-Tac-Toe	10%	-0.30 (0.23)	-8.07 (0.35)	-4.40 (0.25)	<b>-17.24 (0.40)</b>
	20%	-6.72 (0.33)	-18.20 (0.17)	-7.60 (0.12)	<b>-29.90 (0.45)</b>
	30%	-19.50 (0.36)	-25.12 (0.13)	-13.90 (0.41)	<b>-42.85 (0.17)</b>
Breakthrough	10%	-6.53 (0.50)	-18.00 (1.00)	-18.90 (0.36)	<b>-88.73 (1.62)</b>
	20%	-13.67 (0.83)	-30.93 (1.01)	-26.87 (1.03)	<b>-95.87 (1.21)</b>
	30%	-26.33 (1.53)	-42.67 (2.89)	-36.00 (2.65)	<b>-98.33 (1.15)</b>
DouDizhu	10%	-0.25 (1.71)	-18.60 (0.31)	-25.20 (0.76)	<b>-29.94 (0.64)</b>
	20%	-10.45 (1.68)	-24.40 (0.83)	-32.27 (0.69)	<b>-32.87 (0.20)</b>
	30%	-11.29 (1.40)	-28.07 (1.22)	-32.67 (0.20)	<b>-34.54 (0.31)</b>

## S9 Evaluation on Explaining Sub-optimal Agents

As mentioned in Section 4.3, to verify the effectiveness of `StateMask` in terms of explaining sub-optimal agents, we conducted additional experiments on sub-optimal agents in Pong, Kick-And-Defend, Connect 4, and Breakthrough games. These games include both normal-form games (*i.e.*, Pong and Kick-And-Defend) and extensive-form games (*i.e.*, Connect and Breakthrough). Regarding the selection of sub-optimal agents in these four games, we utilized policies from the halfway stage of training as sub-optimal agents in Pong, Connect 4, and Breakthrough. In the Kick-And-Defend game, we follow the setting in Supplement S5.2 and explain the defender. Note that the original zoo model (<https://github.com/openai/multiagent-competition/tree/master/agent-zoo>) offered three different policies for the kicker. We held the defender constant and had each kicker play against the defender separately, recording their corresponding winning rates. The kicker that displayed the lowest winning rate was chosen as the sub-optimal agent.

### S9.1 Fidelity

In this experiment, we compare the fidelity scores of our method and baseline methods across the four selected games. As depicted in Figure 15, our method still achieves the highest fidelity score among the four games even though the target agent is sub-optimal. The reason is that `StateMask` is designed to preserve the original agent’s performance before and after masking the target agent at

Table 5: Results of EDGE’s policy patching method with different explanation methods. Each experiment contains 500 runs. We repeat all experiments three times and report the average reward increase with the corresponding standard deviation in the table below.

Application	Games	EDGE	Value-max	LazyMDP	Ours
Target agent’s winning rate improvement after patching	Kick-And-Defend	+0.00 (0.00)	+0.00 (0.00)	+0.00 (0.00)	+0.00 (0.00)
	You-Shall-Not-Pass	+0.00 (0.00)	+0.75 (0.04)	+0.25 (0.01)	+0.25 (0.02)

Table 6: Additional results of policy patching. Each experiment contains 500 runs. We repeat all experiments three times and report the average reward increase with the corresponding standard deviation in the table below.

Application	Games	EDGE	Value-max	LazyMDP	Ours
Target agent’s winning rate improvement after patching	Kick-And-Defend	+1.03 (0.12)	+0.70 (0.20)	+0.97 (0.06)	+ <b>1.37 (0.12)</b>
	Pendulum	+0.00 (0.00)	+0.29 (0.03)	+2.65 (0.05)	+ <b>4.30 (0.40)</b>
	Tic-Tac-Toe	+0.03 (0.06)	+0.23 (0.06)	+0.20 (0.10)	+ <b>2.47 (0.12)</b>

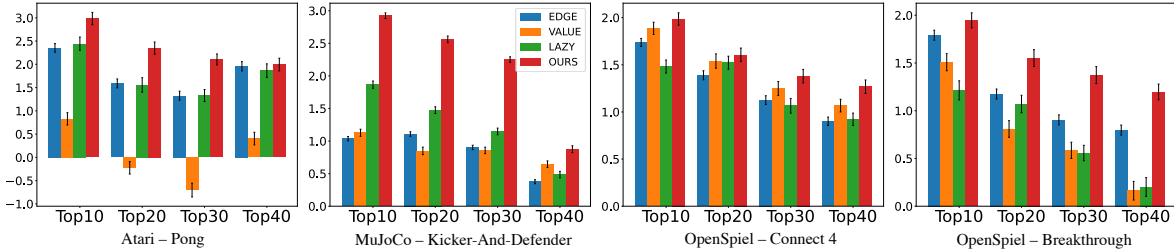


Figure 15: Fidelity scores for interpretations generated by three baseline methods and our proposed explanation method for four sub-optimal agents.

certain time steps. In instances where the target agent is sub-optimal, the important time steps are those that lead the target agent to win or lose (*i.e.*, with a higher chance) in a single episode. Altering the actions in these time steps may cause a significant variation in performance. Therefore, **StateMask** has the potential to recognize and distinguish these critical time steps by learning how to unmask them accurately.

### S9.2 Visualizing the Explanation for Sub-optimal Agent Behaviors

Following Section 5, we also visualize the important time steps identified by **StateMask** in the selected four games to demonstrate **StateMask** could generate human-understandable explanations even for sub-optimal agents.

**Pong.** Regarding the Pong game as Figure 16 shows, our method indicates that the most crucial time step is when the ball is flying towards the yellow paddle. Nevertheless, the yellow paddle moves upward too much when trying to catch the ball. If the yellow paddle takes a different action, *e.g.*, moves downward, the game outcome could be flipped.

**Kick-And-Defend.** In the Kick-And-Defend game, as our explanation method demonstrates in Figure 17, the most critical time step is identified when the kicker is in contact with the ball. As shown in the figure, the kicker’s positioning and approach to the ball lead to a sub-optimal angle for the shot. Consequently, this results in the ball being intercepted easily by the defender, who is well-positioned to block the trajectory. If the kicker were to adjust their angle or approach, the outcome of the game could potentially change, as the ball might bypass the defender, increasing the likelihood of scoring a goal.

**Connect4.** In the Connect 4 game as Figure 18 shows, **StateMask** pinpoints the penultimate step as the most crucial step of the losing trajectory. Once the black player determines to drop his token into the seventh column in the second-to-the-last step, we could observe that no matter which column the black player chooses in the last step, the game outcome will always be a failure. However, if the black player chooses the second column in the second-to-the-last step, he would have a chance to win,

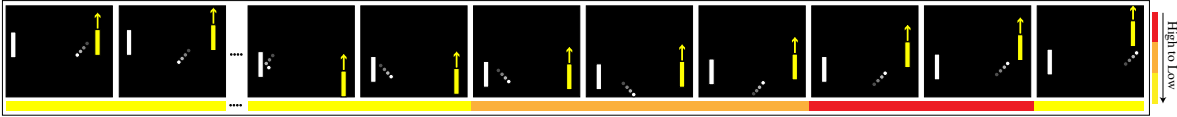


Figure 16: Visualization of the identified critical time steps in the Pong game. The yellow paddle is controlled by the agent we aim to explain.

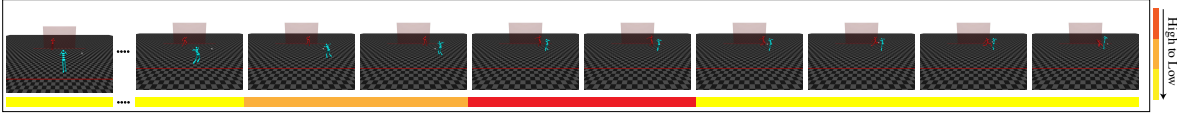


Figure 17: Visualization of the identified critical time steps in the Kick-And-Defend game. The kicker(blue agent) is the agent we target to explain.

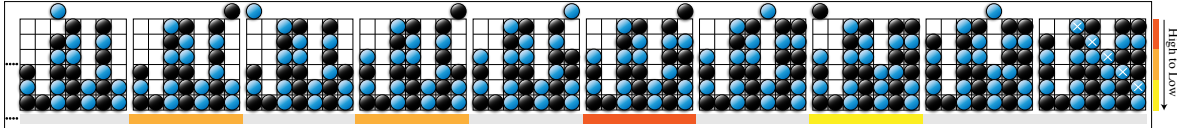


Figure 18: Visualization of the identified critical time steps in Connect 4 game. The black player is the sub-optimal agent we aim to explain.

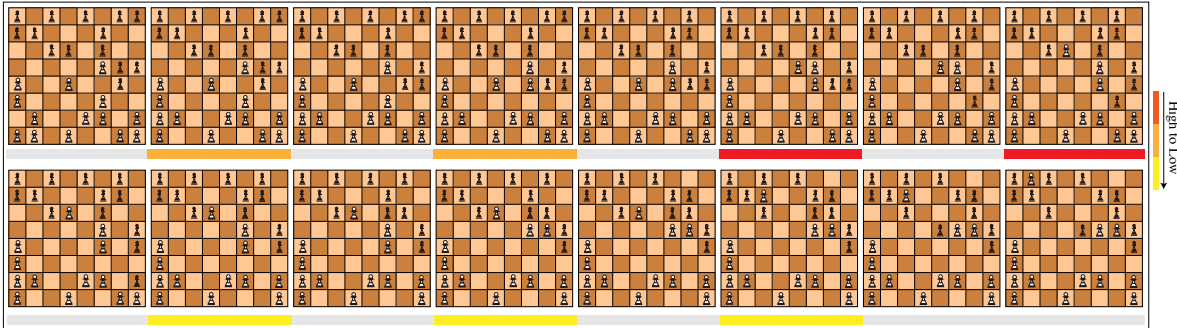


Figure 19: Visualization of the identified critical time steps in the Breakthrough game. The sub-optimal agent plays as the black player and the opponent plays as the white one.

*i.e.*, connecting four tokens between the first column and the fourth column either horizontally or diagonally. Therefore, the second-to-the-last step is the most crucial step in this losing trajectory.

**Breakthrough.** Regarding the Breakthrough game as Figure 19 shows, our method identifies the fifth-to-the-last and the fourth-to-the-last step as the most critical ones. Note that only if the square containing the opponent’s piece is one step diagonally forward may a piece move into and replace it. Apparently, in the fifth-to-the-last step, the black player fails to replace the left white piece in the fourth row, directly causing the game to lose. Additionally, in the fourth-to-the-last step, the black player’s action makes him lose the most advanced piece. The identified two steps are thus the key steps for the black player to lose the game.

### S9.3 Patching Results of Sub-optimal Agents

In this experiment, we follow the retraining method proposed in Section 5 and patch the sub-optimal agents in the selected four games. Table 7 shows the results of the sub-optimal agent performance improvement under the guidance of both **StateMask** and the baseline methods. After retraining, the agents’ performance generally has a large improvement due to these agents being far from optimal. More importantly, retraining based on our explanation achieves the best performance, which indicates the superiority of **StateMask**.

Table 7: Patching results of sub-optimal agents in four games. Each experiment contains 500 runs. We repeat all experiments three times and report the average reward increase with the corresponding standard deviation in the table below.

Application	Games	EDGE	Value-max	LazyMDP	Ours
Target agent’s winning rate improvement after patching	Pong	+5.80 (0.12)	+5.40 (0.03)	+12.00 (1.24)	+ <b>13.60 (1.22)</b>
	Kick-And-Defend	+7.42(0.40)	+8.43(0.24)	+4.78(0.12)	+ <b>10.26(0.62)</b>
	Connect 4	+24.80 (1.68)	+35.80 (1.84)	+36.20 (2.20)	+ <b>37.60(1.66)</b>
	Breakthrough	+68.40 (3.68)	+65.80 (2.77)	+ 68.80 (3.26)	+ <b>69.00 (3.07)</b>

Table 8: Results of relative errors in four selected games. Each experiment contains 500 runs. We repeat all experiments three times and report the mean and standard deviation of the discounted total rewards in the table below.

Games	Pong	Kick-And-Defend	Connect 4	Breakthrough
Sub-optimal agent performance	0.18 (0.00)	0.09 (0.00)	0.52 (0.01)	-0.39 (0.01)
Relative error	<b>StateMask</b>	2.57 (0.03)	5.34 (0.54)	3.05 (0.34)
	<b>PPOMask</b>	3.86 (0.06)	7.53 (0.65)	5.77 (0.42)

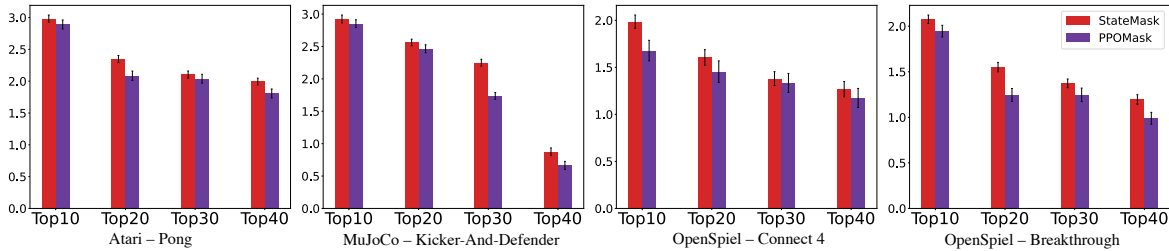


Figure 20: Fidelity comparisons between **StateMask** and **PPOMask** across four selected games when the agent is sub-optimal.

## S10 Evaluation on An Alternative Design

As mentioned in Section 4.3, we examine an alternative design of **StateMask** named as **PPOMask** that trains a mask network by maximizing the masked agent’s expected total reward (*i.e.*,  $J(\theta) = \max_{\theta} \eta(\tilde{\pi}_{\theta})$ ). This is done by directly using the PPO algorithm to train the mask network. To avoid the trivial solution, same as Section 3.2, we also add an additional loss item  $L_t^{\text{MASK}}$  to the PPO loss. We evaluate **PPOMask** in Pong, Kick-And-Defend, Connect 4, and Breakthrough game.

**Relative Error.** Here, we report the relative errors of **PPOMask** in comparison to **StateMask** across these chosen four games. As depicted in Table 8, **PPOMask** generates a higher relative error than **StateMask** when the target agent is sub-optimal, due to its inability to maintain the target agent’s performance (*i.e.*, **PPOMask** trains a masked agent that performs better than the original agent).

**Fidelity.** We also test the fidelity of **PPOMask** and compare it with **StateMask** in these four games. According to Figure 20, **PPOMask** exhibits poor fidelity on sub-optimal agents. This can be attributed to the objective function of **PPOMask**, which is to maximize the expected total reward of a mixed policy. Consequently, **PPOMask** might disregard the critical states that contribute to the failure of the original agent and instead take random actions (*i.e.*, mask operation) during those steps in order to secure a win under the perturbed policy. However, as shown in S9, our method is able to identify the critical states that contribute to the failure of the sub-optimal agent and thus has higher fidelity.

## S11 Potential Social Impact

Our work focuses on improving the trustworthiness of Deep Reinforcement Learning systems, which are increasingly being used in a wide range of applications, from gaming [5] to robotics [8] to healthcare [15].

One of the main challenges of DRL is the black-box nature of the models, which makes it difficult to understand how they arrive at their decisions. This lack of transparency can create concerns about the reliability and safety of DRL systems.

To address this challenge, our work aims to automatically generate explanations for DRL systems, without requiring human supervision. By generating explanations automatically, we reduce the cost and effort required to provide explanations, making them more accessible and scalable for various applications. Moreover, it avoids potential biases that may arise from human-generated explanations, as these may be influenced by subjective factors or an incomplete understanding of the system.

Our approach involves developing models that can analyze the behavior of DRL systems and generate explanations based on that analysis. These explanations provide insights into how the DRL system works, what factors influence its decisions, and how it can be improved. By providing this information, our work contributes to enhancing the transparency and interpretability of DRL systems, which can help users to evaluate the reliability of these systems.

When it comes to the potential negative societal impacts of our work, the use of **StateMask** for enhancing RL agents may lead to the magnification of biased and unfair RL agents. Nevertheless, our method also has the capability of understanding the decision-making process of biased and unfair RL agents, which enables the implementation of strategies to diminish their harmful effects. Therefore, **StateMask** is crucial for understanding and improving RL agents.

## References

- [1] Stephen Boyd, Stephen P Boyd, and Lieven Vandenbergh. *Convex optimization*. Cambridge university press, 2004.
- [2] Yang Guan, Minghuan Liu, Weijun Hong, Weinan Zhang, Fei Fang, Guangjun Zeng, and Yue Lin. Perfectdou: Dominating doudizhu with perfect information distillation. In *Proc. of NeurIPS*, 2022.
- [3] Wenbo Guo, Xian Wu, Usman Khan, and Xinyu Xing. Edge: Explaining deep reinforcement learning policies. In *Proc. of NeurIPS*, 2021.
- [4] Eric Jang, Shixiang Gu, and Ben Poole. Categorical reparameterization with gumbel-softmax. In *Proc. of ICLR*, 2017.
- [5] Guillaume Lample and Devendra Singh Chaplot. Playing fps games with deep reinforcement learning. In *Proc. of AAAI*, volume 31, 2017.
- [6] Marc Lanctot, Edward Lockhart, Jean-Baptiste Lespiau, Vinicius Zambaldi, Satyaki Upadhyay, Julien Pérolat, Sriram Srinivasan, Finbarr Timbers, Karl Tuyls, Shayegan Omidshafiei, et al. Openspiel: A framework for reinforcement learning in games. *arXiv preprint arXiv:1908.09453*, 2019.
- [7] Nicholas Metropolis and Stanislaw Ulam. The monte carlo method. *Journal of the American statistical association*, 44(247):335–341, 1949.
- [8] Farzad Niroui, Kaicheng Zhang, Zhenkai Kashino, and Goldie Nejat. Deep reinforcement learning robot for search and rescue applications: Exploration in unknown cluttered environments. *IEEE Robotics and Automation Letters*, 4(2):610–617, 2019.
- [9] Adam Paszke, Sam Gross, Francisco Massa, Adam Lerer, James Bradbury, Gregory Chanan, Trevor Killeen, Zeming Lin, Natalia Gimelshein, Luca Antiga, et al. Pytorch: An imperative style, high-performance deep learning library. In *Proc. of NeurIPS*, 2019.
- [10] John Schulman, Sergey Levine, Pieter Abbeel, Michael Jordan, and Philipp Moritz. Trust region policy optimization. In *Proc. of ICML*, 2015.
- [11] John Schulman, Filip Wolski, Prafulla Dhariwal, Alec Radford, and Oleg Klimov. Proximal policy optimization algorithms. *arXiv preprint arXiv:1707.06347*, 2017.
- [12] David Silver, Thomas Hubert, Julian Schrittwieser, Ioannis Antonoglou, Matthew Lai, Arthur Guez, Marc Lanctot, Laurent Sifre, Dhharshan Kumaran, Thore Graepel, et al. A general reinforcement learning algorithm that masters chess, shogi, and go through self-play. *Science*, 362(6419):1140–1144, 2018.
- [13] Richard S Sutton. Learning to predict by the methods of temporal differences. *Machine learning*, 3:9–44, 1988.
- [14] Sebastian Thrun. Monte carlo pomdps. In *Proc. of NeurIPS*, 1999.
- [15] Chao Yu, Jiming Liu, Shamim Nemati, and Guosheng Yin. Reinforcement learning in healthcare: A survey. *ACM Computing Surveys (CSUR)*, 55(1):1–36, 2021.
- [16] Daochen Zha, Jingru Xie, Wenye Ma, Sheng Zhang, Xiangru Lian, Xia Hu, and Ji Liu. Douzero: Mastering doudizhu with self-play deep reinforcement learning. In *Proc. of ICML*, 2021.